

## ORIGINAL ARTICLE

WILEY

Diabetes/Lipids/Obesity/Metabolism

# Glucose metabolism and radiodensity of abdominal adipose tissue: A 5-year longitudinal study in a large PET cohort

Kyoungjune Pak<sup>1,2</sup>  | Severi Santavirta<sup>3,4</sup>  | Seunghyeon Shin<sup>5</sup>  |  
Hyun-Yeol Nam<sup>5</sup>  | Sven De Maeyer<sup>6</sup>  | Lauri Nummenmaa<sup>3,4,7</sup> 

<sup>1</sup>Department of Nuclear Medicine and Biomedical Research Institute, Pusan National University Hospital, Busan, Republic of Korea

<sup>2</sup>School of Medicine, Pusan National University, Busan, Republic of Korea

<sup>3</sup>Turku PET Centre, University of Turku, Turku, Finland

<sup>4</sup>Turku University Hospital, Turku, Finland

<sup>5</sup>Department of Nuclear Medicine, Samsung Changwon Hospital, School of Medicine, Sungkyunkwan University, Changwon, Republic of Korea

<sup>6</sup>Department of Training and Education Sciences, Faculty of Social Sciences, University of Antwerp, Antwerp, Belgium

<sup>7</sup>Department of Psychology, University of Turku, Turku, Finland

## Correspondence

Kyoungjune Pak, Department of Nuclear Medicine and Biomedical Research Institute, Pusan National University Hospital, Busan, Republic of Korea.  
Email: [ilikechopin@me.com](mailto:ilikechopin@me.com)

## Funding information

Academy of Finland LN, Grant/Award Numbers: 294897, 332225; Sigrid Juséliuksen Säätiö; Turku University Foundation Grant; State Research Funding for Expert Responsibility Area; National Research Foundation of Korea, Grant/Award Number: 2020R1F1A1054201

## Abstract

**Objective:** <sup>18</sup>F-Fluorodeoxyglucose positron emission tomography/computed tomography (PET/CT) allows noninvasive assessment of glucose metabolism and radiodensity in visceral adipose tissue (VAT) and subcutaneous adipose tissue (SAT). We aimed to address the effects of ageing and metabolic factors on abdominal adipose tissue.

**Design, Patients and Measurements:** We retrospectively analyzed data from 435 healthy men (mean 42.8 years) who underwent a health check-up programme twice, at baseline and the 5-year follow-up. The mean standardized uptake value (SUV) was measured using SAT and VAT and divided by the liver SUV. The mean Hounsfield units (HU) of the SAT and VAT were measured from the CT scans. The effects of clinical variable clusters on SUVR were investigated using Bayesian hierarchical modelling; metabolic cluster (BMI, waist-to-hip ratio, fat percentage, muscle percentage\*–1, HOMA-IR), blood pressure (systolic, diastolic), glucose (fasting plasma glucose level, HbA1c) and C-reactive protein.

**Results:** All the clinical variables changed during the 5-year follow-up period. The SUVR and HU of the VAT increased during follow-up; however, those of the SAT did not change. SUVR and HU were positively correlated with both VAT and SAT. SAT and VAT SUVR were negatively associated with metabolic clusters.

**Conclusions:** Ageing led to increased glucose metabolism and radiodensity in VAT, but not in SAT. VAT may reflect the ageing process more directly than SAT. Glucose metabolism was higher and radiodensity was lower in VAT than in SAT, probably owing to differences in gene expression and lipid density. Both glucose metabolism and radiodensity of VAT and SAT reflect metabolic status.

## KEYWORDS

<sup>18</sup>F-FDG, adipose tissue, glucose metabolism, PET, radiodensity

## 1 | INTRODUCTION

The prevalence of obesity has nearly tripled over the last three decades.<sup>1</sup> Obesity is one of the most critical public health concerns of the 21st century.<sup>1</sup> It is associated with an increased risk of

chronic metabolic diseases such as cardiovascular disease, diabetes, dyslipidemia, hypertension and nonalcoholic fatty liver.<sup>2,3</sup>

Adipose tissue has no specific anatomy.<sup>4</sup> It consists of multiple depots situated in two primary compartments of the body: visceral adipose tissue (VAT) and subcutaneous adipose tissue (SAT). The VAT

is located within the intra-abdominal cavity and is linked to digestive organs, including the omental, mesenteric, and epiploic adipose tissue depots.<sup>4,5</sup> The SAT is located beneath the skin, separated by the abdominal wall, and represents over 80% of the total body fat.<sup>5</sup> However, adipose depots are structured to form large organs with a distinct anatomy, specific vascular and nerve supplies, complex cytology and high physiological plasticity.<sup>6</sup> Furthermore, numerous studies have demonstrated the differences between VAT and SAT in terms of gene expression profiles, cell morphology and association with cardiometabolic diseases.<sup>6</sup> Therefore, inflammation within the VAT and SAT could have varying implications for the risk of cardiometabolic diseases.<sup>7</sup>

<sup>18</sup>F-Fluorodeoxyglucose (FDG) positron emission tomography (PET) allows the noninvasive assessment of glucose metabolic activity and inflammation in the adipose tissue.<sup>8</sup> Moreover, computed tomography (CT) enables the noninvasive evaluation of adipose tissue quality in Hounsfield units (HU).<sup>9</sup> Thus, <sup>18</sup>F-FDG PET/CT is a reliable tool for the simultaneous evaluation of VAT and SAT. Glucose metabolism in VAT is lower in obese participants than in lean participants<sup>10</sup> and lower attenuation of VAT is associated with risk factors for cardiometabolic diseases.<sup>11</sup> However, there has been no investigation of the interaction between glucose metabolism and abdominal adipose tissue radiodensity, the distinctive features of VAT and SAT in terms of glucose metabolism and radiodensity, or the longitudinal changes in VAT and SAT over time. Therefore, to address the effects of ageing and metabolic factors on abdominal adipose tissue, we analyzed a large cohort ( $n = 435$ ) of healthy middle-aged adults (mean 42.8 years) who underwent <sup>18</sup>F-FDG PET/CT scans and a health check-up program twice: at baseline and the 5-year follow-up. We used Bayesian hierarchical modelling to estimate the effects of clinical variables on glucose metabolism and radiodensity of VAT and SAT.

## 2 | PATIENTS AND METHODS

### 2.1 | Participants

We retrospectively analyzed data from 473 healthy male participants who underwent a health checkup programme at Samsung Changwon Hospital Health Promotion Centre between 2013 (baseline) and 2018 (follow-up). After excluding participants with neuropsychiatric disorders ( $n = 5$ ) or malignancies ( $n = 3$ ), those with missing anthropometric and body composition measurements ( $n = 24$ ), or CT ( $n = 6$ ), 435 healthy men were included in both the baseline (mean 42.8, range 38–50 years) and follow-up (mean 48.0, range 43–55 years) studies. The health checkup program included (1) <sup>18</sup>F-FDG PET/CT, (2) anthropometric and body composition measurements and (3) blood samples. The participants in this study were included in a previous study on the effects of ageing on brain glucose metabolism.<sup>12</sup> The study protocol was approved by the Institutional Review Board (Samsung Changwon Medical Centre 2019-06-005-004) and the requirement for informed consent from the participants was waived owing to the retrospective study design.

### 2.2 | <sup>18</sup>F-FDG PET/CT

The participants were asked to avoid strenuous exercise for 24 h and fast for at least 6 h before the PET study. PET/CT was performed 60 min after <sup>18</sup>F-FDG (3.7 MBq/kg) using a Discovery 710 PET/CT scanner (GE Healthcare). Continuous spiral CT was performed with a tube voltage of 120 kVp and tube current of 30–180 mAs. PET scans were obtained in a 3-dimensional mode with a full width at half maximum of 5.6 mm and reconstructed using an ordered subset expectation maximization algorithm. From the PET scans, the mean standardized uptake value (SUV) was measured using a circular region of interest (ROI) from the right lobe of the liver parenchyma, SAT, and VAT at the umbilical level. The standardized uptake value ratio (SUVr) was calculated by dividing the SUV of each ROI by the liver SUV. Using the same ROIs as for the SUV measurement, the mean Hounsfield units (HU) of the SAT and VAT were measured from the CT scans. A representative PET/CT scan with an ROI is shown in Supporting Information S1: Figure 1.

### 2.3 | Body measurement

For anthropometric measurements, height (cm) and weight (kg) were measured and body mass index (BMI) was calculated as  $\text{weight}/\text{height}^2$  ( $\text{kg}/\text{m}^2$ ). Waist and hip circumferences (cm) were measured, and the waist-to-hip ratio was calculated. Commercially available bioelectrical impedance analysis (InBody S10, Biospace) was used to calculate fat percentage (%) and muscle percentage (%) after dividing fat mass (kg) and skeletal muscle mass (kg) by weight (kg). Systolic and diastolic blood pressures (mmHg) and heart rate were measured using an automatic sphygmomanometer (EASY X 800; Jawon Medical Co., Ltd.) after at least 10 min of rest.

### 2.4 | Blood samples

Blood samples were collected from the antecubital vein of each participant. Fasting plasma glucose (mg/dL) and insulin ( $\mu\text{U}/\text{mL}$ ) were measured and homeostatic model assessment for insulin resistance (HOMA-IR) was calculated as follows:  $\text{fasting insulin } (\mu\text{U}/\text{mL}) \times \text{fasting plasma glucose } (\text{mg}/\text{dL}) / 405$ .<sup>13</sup> Haemoglobin A1c (HbA1c, %) levels were analyzed using high-performance liquid chromatography (HPLC).

### 2.5 | Statistical analysis

Normality was tested with the Shapiro–Wilk test and SUVr and HU were log-transformed after adding 130 to HU as the minimum HU was  $-129$  (baseline VAT). Comparisons of clinical variables and SUVr between baseline and follow-up were performed using paired  $t$ -tests. Pearson's correlation coefficient was used to determine the association between SUVr and HU.

**TABLE 1** Participant characteristics.

		Baseline study	5-year follow-up	<i>p</i>
Age		42.8 ± 3.6	48.0 ± 3.6	<.0001
Metabolic cluster	Body mass index (kg/m <sup>2</sup> )	24.7 ± 2.9	24.9 ± 2.8	.0002
	Waist-hip ratio	0.89 ± 0.03	0.89 ± 0.04	<.0001
	Fat percentage (%)	23.1 ± 5.2	23.5 ± 5.2	.0022
	Muscle percentage (%) <sup>a</sup> -1	-43.3 ± 3.0	-43.1 ± 3.0	.0002
	HOMA-IR	1.2 ± 0.8	1.8 ± 1.2	<.0001
Blood pressure	Systolic (mmHg)	120.3 ± 11.0	122.6 ± 11.0	<.0001
	Diastolic (mmHg)	72.8 ± 9.5	76.6 ± 9.1	<.0001
Glucose	Fasting plasma glucose (mg/dL)	93.0 ± 16.6	101.8 ± 23.6	<.0001
	HbA1c (%)	5.6 ± 0.6	5.7 ± 0.7	<.0001
C-reactive protein (mg/dL)		1.1 ± 1.8	1.3 ± 3.0	.2450

Abbreviation: HOMA-IR, homeostatic model assessment for insulin resistance.

<sup>a</sup>mean ± standard deviation.

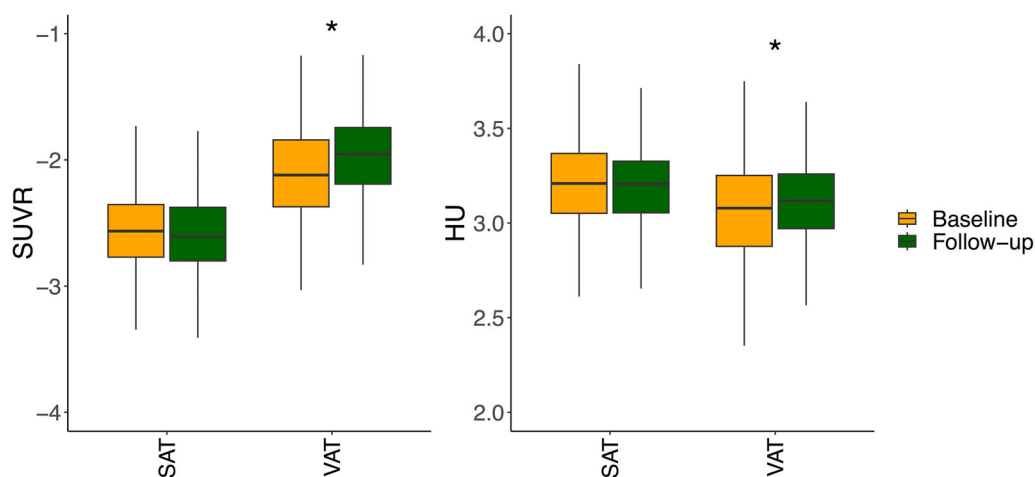


**FIGURE 1** Comparison between baseline and follow-up studies: VAT SUVR ( $p < .0001$ ) and VAT HU ( $p = .0094$ ) increased during the 5-year follow-up; however, SAT SUVR ( $p = .2181$ ) and SAT HU ( $p = .2697$ ) did not change significantly. HU, Hounsfield units; SAT, subcutaneous adipose tissue; SUVR, standardized uptake value ratio; VAT, visceral adipose tissue. [Color figure can be viewed at [wileyonlinelibrary.com](https://onlinelibrary.wiley.com/terms-and-conditions)]

### 2.5.1 | Cluster analysis for predictor variables

Because the clinical variables contained missing values (baseline study: HOMA-IR 35/435), we used a nonparametric imputation algorithm, missForest, with default parameters for the imputation of the missing values.<sup>14</sup> As some clinical variables were correlated, we used hierarchical clustering analysis before Bayesian hierarchical modelling.<sup>12</sup> Before clustering, the muscle percentage was multiplied by -1 to simplify the solution, as it was the only variable that showed negative correlations with the other predictors. Clustering yielded stable cluster hierarchy across the six tested algorithms (complete-linkage, single-linkage, UPGMA, WPGMA, WPGMC and Ward) and the following clusters were defined (1) metabolic cluster

(BMI, waist-to-hip ratio, fat percentage, muscle percentage\*-1, HOMA-IR), (2) blood pressure (systolic, diastolic), (3) glucose (fasting plasma glucose, HbA1c) and (4) C-reactive protein (CRP). In each cluster, the values were calculated after averaging the standardized clinical variables (Supporting Information S1: Figure 2).

### 2.5.2 | Bayesian hierarchical modeling

The effects of clinical clusters on SUVR and HU were investigated using Bayesian hierarchical modelling with brms<sup>15-17</sup> that applies the Markov chain Monte Carlo sampling tools of RStan.<sup>18</sup> We set up a separate model with SUVR or HU as the dependent variable

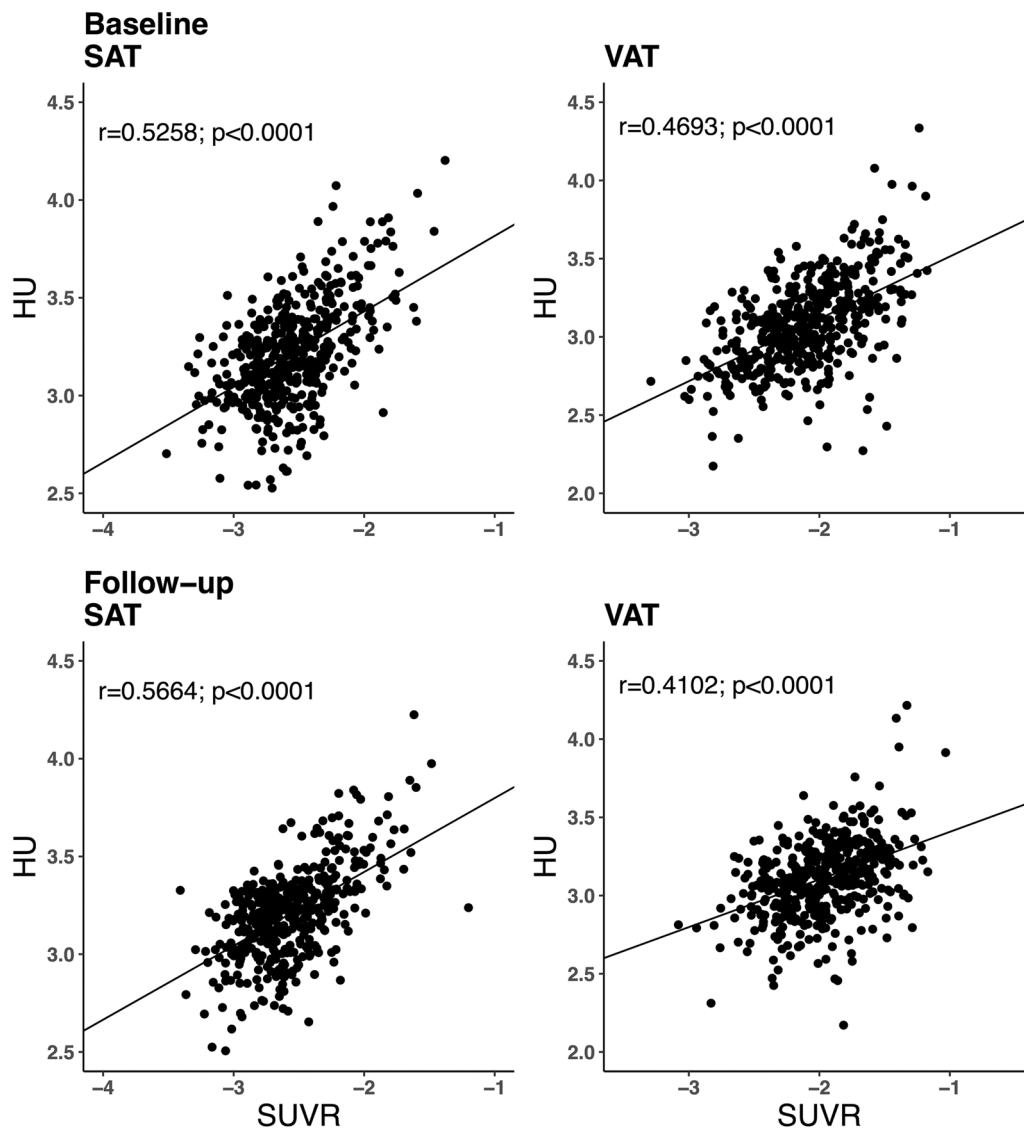


**FIGURE 2** Correlation between SUVR and HU of SAT and VAT in baseline and follow-up studies: SUVR and HU were positively correlated in baseline (SAT,  $r = .5258$ ,  $p < .0001$ ; VAT,  $r = .4693$ ,  $p < .0001$ ) and follow-up (SAT,  $r = .5664$ ,  $p < .0001$ ; VAT,  $r = .4102$ ,  $p < .0001$ ) studies. HU, Hounsfield units; SAT, subcutaneous adipose tissue; SUVR, standardized uptake value ratio; VAT, visceral adipose tissue.

and the four clusters (metabolic, blood pressure, glucose and CRP) as predictors. These fixed effects were calculated individually and as interactions over time. We added participants and ROI as random intercepts to allow SUVR or HU to vary between participants and ROIs and calculated the fixed effects, including the interactions with time, separately for each ROI as a random slope. The Bayesian models were estimated using four Markov chains, each of which had 4000 iterations, including 1000 warm-ups, totalling 12,000 post-warm-up samples. The sampling parameters were modified slightly to facilitate convergence (maximum tree depth = 20). Statistical analyses were performed using R Statistical Software (The R Foundation for Statistical Computing).

### 3 | RESULTS

The participant characteristics are summarized in Table 1. Except for CRP ( $p = .2450$ ), all the clinical variables were increased during the 5-year follow-up; BMI ( $p = .0002$ ), waist-hip ratio ( $p < .0001$ ), fat percentage ( $p = .0022$ ), muscle percentage\*–1 ( $p = .0002$ ), HOMA-IR ( $p < .0001$ ), systolic blood pressure ( $p < .0001$ ), diastolic blood pressure ( $p < .0001$ ), fasting plasma glucose ( $p < .0001$ ) and HbA1c ( $p < .0001$ ) (Supporting Information S1: Figure 3). The VAT SUVR ( $p < .0001$ ) and VAT HU ( $p = .0094$ ) increased during the 5-year follow-up; however, the SAT SUVR ( $p = .2181$ ) and SAT HU ( $p = .2697$ ) did not change significantly (Figure 1). SUVR and HU were positively correlated at baseline (SAT,  $r = .5258$ ,  $p < .0001$ ; VAT,

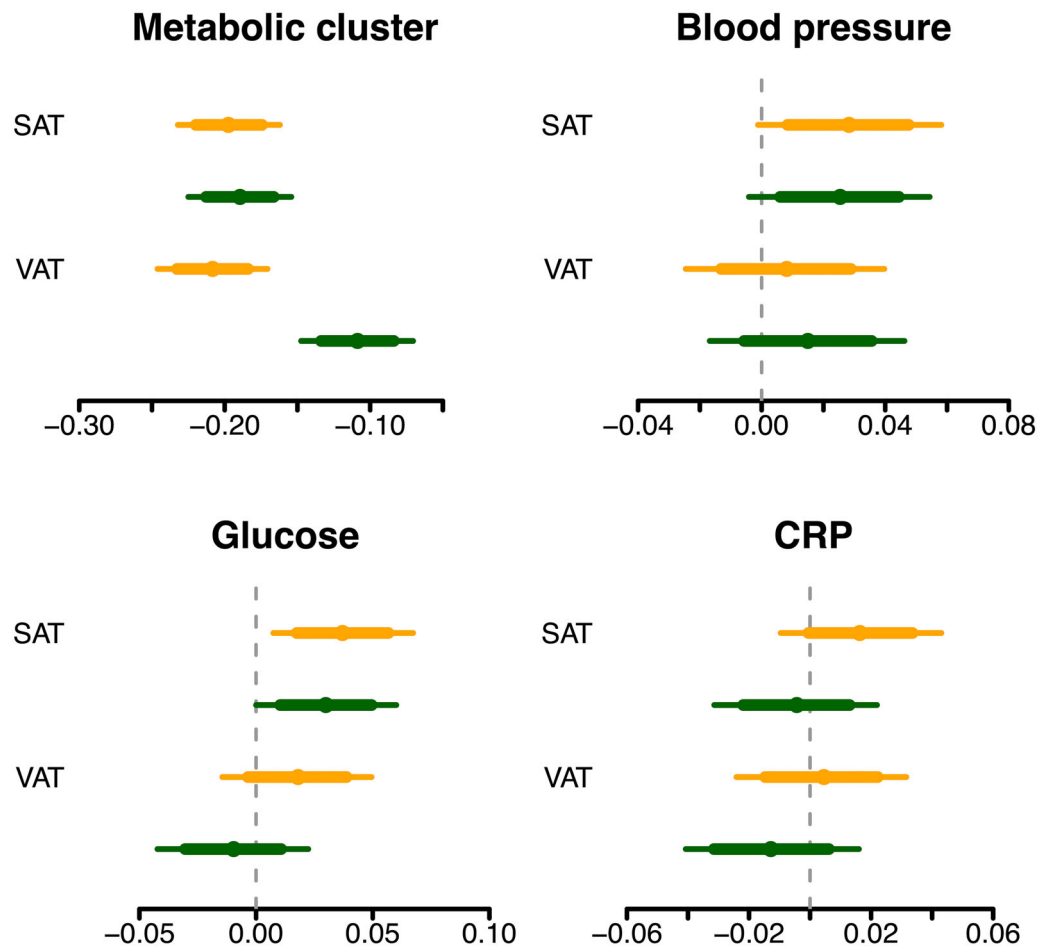


**FIGURE 3** Posterior intervals of the regression coefficients for each cluster predicting SUVR. Thick lines represent the 80% posterior intervals, thin lines represent the 95% posterior intervals, and the circles represent posterior median. CRP, C-reactive protein; SUVR, standardized uptake value ratio. [Color figure can be viewed at [wileyonlinelibrary.com](http://wileyonlinelibrary.com)]

$r = .4693$ ,  $p < .0001$ ) and follow-up (SAT,  $r = .5664$ ,  $p < .0001$ ; VAT,  $r = .4102$ ,  $p < .0001$ ) (Figure 2). The VAT SUVR was higher than the SAT SUVR, while the VAT HU was lower than the SAT HU in both baseline and follow-up studies (all  $p < .0001$ ). The effects of clinical variables on SUV and HUs were generally similar between baseline and follow-up studies. SAT and VAT SUVR were negatively associated with metabolic clusters. The SAT SUVR was positively associated with blood pressure and glucose levels. The effects of CRP markedly overlapped with zero in both the SAT and VAT analyses (Figure 3). Both SAT and VAT HU were negatively associated with metabolic clusters. However, the effects of blood pressure, glucose and CRP markedly overlapped with zero for both SAT and VAT (Figure 4).

## 4 | DISCUSSION

Our main finding was that ageing led to increased glucose metabolism and radiodensity in VAT, but not in SAT. In both VAT and SAT, glucose metabolism and radiodensity were positively

correlated. Glucose metabolism was higher and radiodensity was lower in VAT than in SAT. Both glucose metabolism and the radiodensity of VAT and SAT were negatively associated with the metabolic cluster. Both glucose metabolism and SAT radiodensity were positively associated with glucose levels. The effects of the clinical variables on glucose metabolism and radiodensity were generally similar in the baseline and follow-up studies.

### 4.1 | VAT and SAT

VAT and SAT constitute the two primary fat compartments linked to several cardiometabolic diseases.<sup>19</sup> However, they exhibit distinct functions and characteristics.<sup>5</sup> The VAT is located within the intra-abdominal cavity and can engage in dynamic communication with neighbouring internal organs.<sup>5</sup> In turn, the SAT is located beneath the skin, separated by the abdominal wall and provides protection against physical damage.<sup>5</sup> VAT tends to exhibit proinflammatory characteristics. A certain portion of visceral adipogenic progenitor (APs) cells lose their adipogenic potential and are transformed into

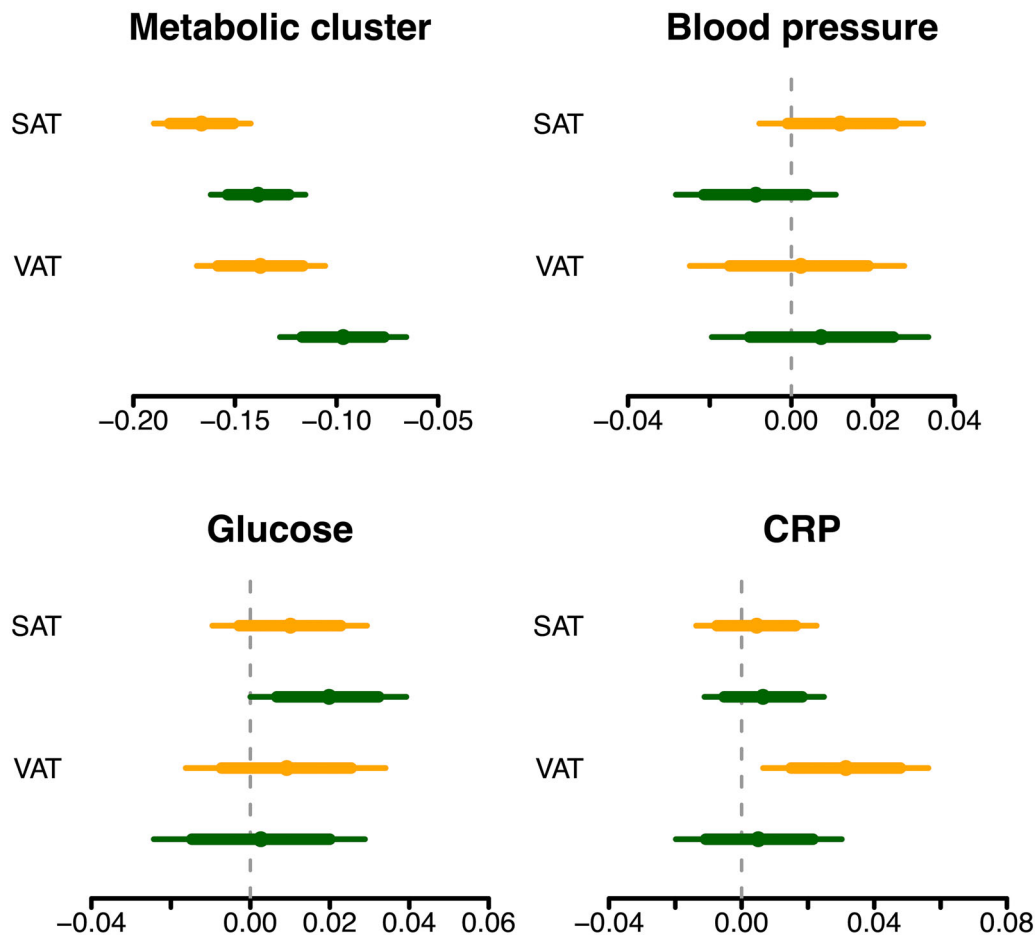


**FIGURE 4** Posterior intervals of the regression coefficients for each cluster predicting HU. Thick lines represent the 80% posterior intervals, thin lines represent the 95% posterior intervals, and the circles represent posterior median. CRP, C-reactive protein; HU, Hounsfield units. [Color figure can be viewed at [wileyonlinelibrary.com](http://wileyonlinelibrary.com)]

proinflammatory fibrocytes, which exacerbate adipose tissue inflammation by inducing fibrosis and secreting proinflammatory cytokines such as tumour necrosis factor- $\alpha$ , interleukin-6 and monocyte chemoattractant protein-1.<sup>20</sup> In contrast, the SAT is less susceptible to inflammatory responses during obesity. Subcutaneous adipogenic progenitors inhibit the infiltration of proinflammatory macrophages into the SAT in response to gamma-aminobutyric acid, which plays a crucial role in suppressing SAT in obesity.<sup>21</sup>

<sup>18</sup>F-FDG PET allows the noninvasive assessment of glucose metabolic activity and inflammation in adipose tissues.<sup>8</sup> Further, CT enables the noninvasive assessment of fat quality in HU.<sup>9</sup> Thus, <sup>18</sup>F-FDG PET/CT is a reliable tool for the evaluation of VAT and SAT with these two modalities at once. VAT SUVR is lower in obese participants than in lean participants<sup>10</sup> and lower VAT HU is associated with an increased risk of hypertension, insulin resistance and metabolic syndrome.<sup>11</sup> In contrast, SAT SUVR is not different between obese and lean participants<sup>10</sup> and a lower SAT HU is associated with a decreased risk of diabetes and cardiometabolic risk factors.<sup>11</sup> In the present study, VAT SUVR was higher than SAT SUVR, whereas VAT HU was lower than SAT HU. As FDG is an analogue of glucose, the significantly higher expression of the hexokinase-1 gene in VAT might be the underlying mechanism for this

difference in glucose metabolism between VAT and SAT.<sup>8</sup> A lower HU value in the VAT represents more lipid-dense fat tissue.<sup>22</sup> Adipose tissue with higher HU values has been associated with smaller adipocytes, probably because of the extracellular matrix of the adipose tissue.<sup>23</sup> A larger adipocyte size may indicate an inability to generate new adipocytes and is linked to insulin resistance.<sup>24</sup> Moreover, a lower VAT HU may indicate a relative lack of vascularity, as blood has a higher HU than adipose tissue on CT.<sup>25</sup> Therefore, VAT might have higher glucose metabolism, higher lipid density and less vascularity than SAT.

## 4.2 | Ageing effect

Physiological changes occur with ageing in the brain and body organs. Adiposity develops between the third and seventh decades of life and increased VAT accumulation is strongly linked to ectopic fat deposition in the skeletal muscle, heart, liver, pancreas and blood arteries.<sup>26</sup> Additionally, the heart and blood vessels become stiffer, causing the blood pressure to be increased.<sup>27</sup> Impaired insulin sensitivity and an increased risk of insulin resistance lead to increased fasting plasma glucose and HbA1c.<sup>28</sup> In this study, all clinical variables except CRP

increased during the 5-year follow-up period: BMI, waist-hip ratio, fat percentage, muscle percentage<sup>-1</sup>, HOMA-IR, blood pressure, fasting plasma glucose and HbA1c, similar to previous longitudinal studies.<sup>29</sup> This shows that the ageing process is a transition towards the loss of metabolic homeostasis and plasticity in middle adulthood. Ageing also led to an increase in VAT SUVR and VAT HU without a change in SAT SUVR or SAT HU. Therefore, VAT may reflect the ageing process more directly than SAT because SAT did not show significant changes in the ageing process in this study.

### 4.3 | Glucose metabolism, radiodensity and clinical variables

Inflammatory cells demonstrate elevated affinity of glucose transporters for deoxyglucose, as well as elevated expression of glucose transporters.<sup>30</sup> Therefore, <sup>18</sup>F-FDG PET is used to diagnose infection and inflammation in clinical setting.<sup>30</sup> However, contrary to our expectations, both VAT SUVR and SAT SUVR were negatively associated with the metabolic cluster. Insulin-resistant adipocytes may outweigh FDG uptake from the inflammation of VAT and SAT.<sup>8</sup> In addition, a lower SUVR may indicate abnormal perfusion, vascular function and capillary density of the VAT and SAT in the higher metabolic cluster.<sup>31</sup> SUVR and HU were positively correlated with each other, and the effects of the clinical variables were generally similar for both SUVR and HU. Therefore, both the SUVR and HU of VAT and SAT strongly reflect the metabolic status of the body. In addition to the metabolic cluster, the glucose cluster was positively associated with the SUVR and HU of SAT, but not with those of VAT. This was unexpected because the effect of the glucose cluster was opposite to that of the metabolic cluster. Until now, the impact of glucose levels on FDG uptake has been investigated in body organs such as the lungs, bone marrow, spleen, bowel and stomach,<sup>32</sup> not in abdominal adipose tissue. FDG uptake in adipose tissue from the upper back showed a positive correlation with the glucose level,<sup>33</sup> however, a study by Büsing et al.<sup>34</sup> showed a negligible change in FDG uptake in adipose tissue (area not specified) that was not influenced by the glucose level.

### 4.4 | Limitations

Only men were included in this study; therefore, the results may not be directly generalizable to women. Furthermore, this retrospective study was based on a health checkup program. However, the mechanisms underlying these findings are not fully understood.

## 5 | CONCLUSIONS

Ageing led to increased glucose metabolism and radiodensity in VAT, but not in SAT. VAT may reflect the ageing process more directly than SAT. Glucose metabolism was higher and radiodensity was lower in VAT than in SAT, probably because of differences in gene

expression and lipid density. Both glucose metabolism and radiodensity of VAT and SAT reflect the metabolic status of the body.

### ACKNOWLEDGEMENTS

This study was supported by the National Research Foundation of Korea (KP: 2020R1F1A1054201), Sigrid Juselius Foundation (LN), Academy of Finland (LN: 294897 and 332225), Turku University Foundation Grant (SS) and State Research Funding for Expert Responsibility Area (ERVA) of TYKS (SS).

### CONFLICT OF INTEREST STATEMENT

The authors declare no conflict of interest.

### DATA AVAILABILITY STATEMENT

The datasets used and/or analyzed in the current study are available from the corresponding author upon reasonable request.

### ORCID

Kyoungjune Pak  <http://orcid.org/0000-0001-5051-1894>  
 Severi Santavirta  <http://orcid.org/0000-0001-7538-9549>  
 Seunghyeon Shin  <http://orcid.org/0000-0002-9679-1569>  
 Hyun-Yeol Nam  <https://orcid.org/0000-0003-2995-1961>  
 Sven De Maeyer  <http://orcid.org/0000-0003-2888-1631>  
 Lauri Nummenmaa  <http://orcid.org/0000-0002-2497-9757>

### REFERENCES

1. Agha M, Agha R. The rising prevalence of obesity: part A: impact on public health. *Int J Surg Oncol*. 2017;2(7):e17.
2. Eisenstein SA, Bischoff AN, Gredysa DM, et al. Emotional eating phenotype is associated with central dopamine D2 receptor binding independent of body mass index. *Sci Rep*. 2015;5:11283.
3. Flegal K, Carroll M, Kuczmarski R, Johnson C. Overweight and obesity in the United States: prevalence and trends, 1960-1994. *Int J Obes*. 1998;22(1):39-47.
4. Passaro A, Miselli MA, Sanz JM, et al. Gene expression regional differences in human subcutaneous adipose tissue. *BMC Genomics*. 2017;18(1):202.
5. Hwang I, Kim JB. Two faces of White adipose tissue with heterogeneous adipogenic progenitors. *Diabetes Metab J*. 2019;43(6):752-762.
6. Cinti S. The adipose organ at a glance. *Dis Models & Mech*. 2012;5(5): 588-594.
7. Tahara N, Yamagishi S, Kodama N, et al. Clinical and biochemical factors associated with area and metabolic activity in the visceral and subcutaneous adipose tissues by FDG-PET/CT. *J Clin Endocrinol Metab*. 2015;100(5):E739-E747.
8. Christen T, Sheikine Y, Rocha VZ, et al. Increased glucose uptake in visceral versus subcutaneous adipose tissue revealed by PET imaging. *JACC: Cardiovascular Imaging*. 2010;3(8):843-851.
9. Rosenquist KJ, Massaro JM, Pedley A, et al. Fat quality and incident cardiovascular disease, all-cause mortality, and cancer mortality. *J Clin Endocrinol Metab*. 2015;100(1):227-234.
10. Oliveira AL, Azevedo DC, Bredella MA, Stanley TL, Torriani M. Visceral and subcutaneous adipose tissue FDG uptake by PET/CT in metabolically healthy obese subjects. *Obesity*. 2015;23(2): 286-289.
11. Rosenquist KJ, Pedley A, Massaro JM, et al. Visceral and subcutaneous fat quality and cardiometabolic risk. *JACC: Cardiovasc Imaging*. 2013;6(7): 762-771.

12. Pak K, Malén T, Santavirta S, et al. Brain glucose metabolism and aging: a 5-Year longitudinal study in a large positron emission tomography cohort. *Diabetes Care*. 2023;46(2):e64-e66.
13. Matthews DR, Hosker JP, Rudenski AS, Naylor BA, Treacher DF, Turner RC. Homeostasis model assessment: insulin resistance and  $\beta$ -cell function from fasting plasma glucose and insulin concentrations in man. *Diabetologia*. 1985;28(7):412-419.
14. Stekhoven DJ, Bühlmann P. MissForest--non-parametric missing value imputation for mixed-type data. *Bioinformatics*. 2012;28(1):112-118.
15. Bürkner P-C. Bayesian item response modeling in R with brms and stan. *J Stat Softw*. 2021;100(5):1-54.
16. Bürkner P-C. brms: an R package for Bayesian multilevel models using stan. *J Stat Softw*. 2017;80(1):1-28.
17. Bürkner P-C. Advanced Bayesian multilevel modeling with the R package brms. *The R Journal*. 2018;10(1):395-411.
18. Stan Development Team. RStan: the R interface to Stan. 2022; <https://mc-stan.org/>
19. Fox CS, Massaro JM, Hoffmann U, et al. Abdominal visceral and subcutaneous adipose tissue compartments: association with metabolic risk factors in the framingham heart study. *Circulation*. 2007;116(1):39-48.
20. Weisberg SP, McCann D, Desai M, Rosenbaum M, Leibel RL, Ferrante Jr. AW. Obesity is associated with macrophage accumulation in adipose tissue. *J Clin Invest*. 2003;112(12):1796-1808.
21. Hwang I, Jo K, Shin KC, et al. GABA-stimulated adipose-derived stem cells suppress subcutaneous adipose inflammation in obesity. *Proc Natl Acad Sci*. 2019;116(24):11936-11945.
22. Wronska A, Kmiec Z. Structural and biochemical characteristics of various White adipose tissue depots. *Acta Physiologica*. 2012;205(2):194-208.
23. Murphy RA, Register TC, Shively CA, et al. Adipose tissue density, a novel biomarker predicting mortality risk in older adults. *J Gerontol: Series A*. 2014;69(1):109-117.
24. Weyer C, Foley JE, Bogardus C, Tataranni PA, Pratley RE. Enlarged subcutaneous abdominal adipocyte size, but not obesity itself, predicts type II diabetes independent of insulin resistance. *Diabetologia*. 2000;43(12):1498-1506.
25. Pasarica M, Sereda OR, Redman LM, et al. Reduced adipose tissue oxygenation in human obesity. *Diabetes*. 2009;58(3):718-725.
26. Kuk JL, Saunders TJ, Davidson LE, Ross R. Age-related changes in total and regional fat distribution. *Ageing Res Rev*. 2009;8(4):339-348.
27. Buford TW. Hypertension and aging. *Ageing Res Rev*. 2016;26:96-111.
28. Shou J, Chen PJ, Xiao WH. Mechanism of increased risk of insulin resistance in aging skeletal muscle. *Diabetol Metab Syndr*. 2020;12:14.
29. Lee JJ, Pedley A, Hoffmann U, Massaro JM, Fox CS. Association of changes in abdominal fat quantity and quality with incident cardiovascular disease risk factors. *J Am Coll Cardiol*. 2016;68(14):1509-1521.
30. Love C, Tomas MB, Tronco GG, Palestro CJ. FDG PET of infection and inflammation. *Radiographics*. 2005;25(5):1357-1368.
31. Gealekman O, Guseva N, Hartigan C, et al. Depot-specific differences and insufficient subcutaneous adipose tissue angiogenesis in human obesity. *Circulation*. 2011;123(2):186-194.
32. Lindholm H, Brolin F, Jonsson C, Jacobsson H. The relation between the blood glucose level and the FDG uptake of tissues at normal PET examinations. *EJNMMI Res*. 2013;3(1):50.
33. Sharma P, Chatterjee P, Alvarado LA, Dwivedi AK. Standardized uptake value of normal organs on routine clinical [18F]FDG PET/CT: impact of tumor metabolism and patient-related factors. *Nucl Med Rev Central & Eastern Europe*. 2023;26(0):1-10.
34. Büsing KA, Schönberg SO, Brade J, Wasser K. Impact of blood glucose, diabetes, insulin, and obesity on standardized uptake values in tumors and healthy organs on 18F-FDG PET/CT. *Nucl Med Biol*. 2013;40(2):206-213.

## SUPPORTING INFORMATION

Additional supporting information can be found online in the Supporting Information section at the end of this article.

**How to cite this article:** Pak K, Santavirta S, Shin S, Nam H-Y, De Maeyer S, Nummenmaa L. Glucose metabolism and radiodensity of abdominal adipose tissue: a 5-year longitudinal study in a large PET cohort. *Clin Endocrinol*. 2024;1-8. doi:10.1111/cen.15121